An Analysis of Long Baseline Radio Interferometry

J. B. Thomas
Tracking and Orbit Determination Section

The VLBI (very long baseline interferometer) cross-correlation procedure is analyzed for both a natural point source and a completely incoherent extended source. The analysis is based on a plane wave description of a radio signal that consists of stationary random noise. A formulation of the time delay is developed on the basis of plane wave phase. A brief discussion is devoted to small time delay corrections that are generated by relativistic differences in clock rates in the various coordinate frames. The correlation analysis, which includes electronic factors such as amplitude and phase modulation and the heterodyne process, leads to expressions for fringe amplitude and fringe phase. It is shown that the cross-correlation function for an extended source is identical to the point-source expression if one adjusts the fringe amplitude to include the transform of the brightness distribution. Examples of diurnal paths in the u-v plane are presented for various baselines and source locations. Finally, delay and delay rate measurement accuracy is briefly discussed.

I. Introduction

In very long baseline interferometer (VLBI) measurements, the radio signal produced by a distant source is recorded simultaneously at two radio antennas. Because of a difference in raypaths, the signal will be delayed in time at one antenna relative to the other. By cross-correlating the two signals, the time delay and/or its time derivative may be determined. In addition, correlated amplitude measurements can yield source strength and structure. If the radio signal is generated by an extragalactic object, the radio source may be regarded as a fixed object because of its great distance. In this case, the time dependence of the time delay is generated by the Earth's motion but depends, of course, on the source location and the baseline vector between the two antennas. In general, measurement of the time delay and/or its derivative for many sources can lead to a least-squares determination of source locations, the baseline vector, and Earth motion parameters, such as UT1 and polar motion.

The goal of this report is a systematic analysis that includes the most important features of analog VLBI cross-correlation. The correlation analysis is presented for both a point source and a completely incoherent extended source. The analysis differs from previous work (Refs. 1–5) in several ways. First, the derivation is based on a plane

wave description of the radio noise. This approach allows the time delay and the brightness transform to enter the cross-correlation equations in a natural fashion. Second, the analysis includes a treatment of the relativistic correction to the time delay due to the difference in time scales in the various coordinate frames. Third, statistical averages are made by means of ensemble averages rather than the cross-correlation integral (Ref. 1). The ensemble average approach explicitly bases the derivation on stationarity of the radio noise. Fourth, the derivation includes a model for the electronics which explicitly incorporates the interplay between passband and doppler shift. In particular, the model can lead to the dependence of fringe amplitude and fringe frequency on doppler shifting in the two passbands. Finally, based on the assumption of nearly identical systems, it is shown that all sinusoidal time dependence is relegated to the fast fringes if the effective center frequency is chosen to be the centroid of the doppler-corrected bandpass product. Even though transmission media effects are usually important in VLBI measurements, they have been omitted in this report in order to concentrate on the cross-correlation procedure.

The report includes four major sections. In *Section II*, the time delay for a point source is derived by means of the plane wave phase. The resultant delay equation is developed in order to sketch the contributions of polar motion, aberration, precession, nutation, and diurnal rotation. In *Section III*, the cross-correlation function is derived for a natural point source. In *Section IV*, the cross-correlation function is derived for a completely incoherent extended source. In *Section V*, VLBI measurement uncertainty is briefly discussed.

II. Geometric Time Delay for a Point Source

Typical extragalactic radio sources emit noise waves with a wide frequency distribution. Consider one member of an ensemble of noise waves that could be transmitted by an extragalactic point source. The wave may be represented as a superposition of plane waves in the form

$$E(\mathbf{x}, t) = \int_{-\infty}^{\infty} A(\omega) \exp[i(\omega t - \mathbf{k}\cdot\mathbf{x})]\, d\omega \qquad (1)$$

where E is the electric field at time t and point $\mathbf{x}$, $\mathbf{k}$ is the apparent wave vector of the plane wave and gives the apparent direction of propagation, and $A(\omega)$ is the Fourier amplitude at frequency ω. As usual, $\mathbf{k} = \omega\hat{k}/c$. All quantities are measured with respect to a "quasi-Lorentzian" geocentric (QLG) frame, such as true equatorial coordinates of date. The term "apparent wave vector" refers to the annual aberration effect that will be observed in a QLG frame and will be discussed below. For simplicity, the wave is assumed to be polarized. We will also assume in this derivation that the wave propagates in a vacuum and will not include transmission media effects.

Relative to the QLG frame, the electric fields at the two stations become

$$E_1(t) = E(\mathbf{x}_1(t), t) = \int_{-\infty}^{\infty} A(\omega) \exp[i(\omega t - \mathbf{k}\cdot\mathbf{x}_1(t))]\, d\omega \qquad (2)$$

$$E_2(t) = E(\mathbf{x}_2(t), t) = \int_{-\infty}^{\infty} A(\omega) \exp[i(\omega t - \mathbf{k}\cdot\mathbf{x}_2(t))]\, d\omega \qquad (3)$$

where $\mathbf{x}_1(t)$ and $\mathbf{x}_2(t)$ give the locations of the two stations as a function of time in QLG coordinates as indicated in Fig. 1.

Let a particular segment of the wave reach station 1 at time t_1. This segment will reach station 2 at time t_2 when the following phase equality is satisfied.

$$\mathbf{k}\cdot\mathbf{x}_1(t_1) - \omega t_1 = \mathbf{k}\cdot\mathbf{x}_2(t_2) - \omega t_2 \qquad (4)$$

Let $t_2 = t_1 + \tau_g$ where τ_g is the time delay measured by observers in the QLG frame. Since τ_g will be small ($\lesssim 0.02$ sec for Earth-based antennas), expand about t_1 to obtain

$$\mathbf{x}_2(t_2) = \mathbf{x}_2(t_1) + \mathbf{v}_2(t_1)\,\tau_g \qquad (5)$$

Then one obtains from Eq. (4)

$$\tau_g(t_1) = -\frac{\hat{S}\cdot\mathbf{B}(t_1)}{c}\left[1 + \frac{\hat{S}\cdot\mathbf{v}_2(t_1)}{c}\right]^{-1} \qquad (6)$$

where $\hat{S}$ is a unit vector in the apparent direction of the source given by

$$\hat{S} = \frac{-\mathbf{k}}{|\mathbf{k}|} \qquad (7)$$

$\mathbf{B}$ is the baseline vector given by

$$\mathbf{B}(t_1) = \mathbf{x}_2(t_1) - \mathbf{x}_1(t_1) \qquad (8)$$

As one would expect, the time delay is simply the instantaneous path difference divided by the speed of light with a small correction for the motion of station 2 during the wave transit.

The content of the time delay function will now be outlined in order to illustrate the presence of factors such as precession, nutation, aberration, polar motion and diurnal rotation. The time delay expression in Eq. (6) is most conveniently evaluated in terms of true equatorial coordinates of date. In this coordinate frame, the z-axis is aligned with the instantaneous spin axis of the Earth, and the x-axis is given by the true equinox of date. The apparent source direction $\hat{S}$ and the baseline vector $\mathbf{B}(t)$ may be expressed in terms of this coordinate system in the following manner.

Source positions are typically recorded in terms of right ascension and declination relative to the mean equator and equinox of 1950.0 and must be transformed to coordinates of date. In addition, these recorded source positions refer to the position that would be seen by an inertial observer. Since the source direction contained in the time delay expression is referenced to a geocentric frame, the inertial source position must be adjusted for aberration (Ref. 6) due to the Earth's orbital motion. We will calculate annual aberration in the 1950 frame and then transform to true equatorial coordinates of date.

Suppose $\hat{S}_{50}$ denotes the inertial source direction in 1950 coordinates and is given by

$$\hat{S}_{50} = (\cos\delta_s \cos\alpha_s, \cos\delta_s \sin\alpha_s, \sin\delta_s) \tag{9}$$

where δ_s, α_s are the right ascension and declination relative to the mean equator and equinox of 1950.0. Let $\mathbf{v}_{50}$ denote the Earth's orbital velocity at the time of interest relative to the 1950 frame. If we neglect terms of the order of $v^2/c^2 \approx 10^{-12}$, the aberration-corrected source direction $\hat{S}_c$ in 1950 coordinates is given by (Ref. 6):

$$\hat{S}_c = \mathbf{S}_I/|\mathbf{S}_I| \tag{10}$$

where

$$S_I = \hat{S}_{50} + \mathbf{v}_{50}/c$$

We must now transform $\hat{S}_c$ to true equatorial coordinates of date. If R_{pn} represents the rotation matrix that precesses and nutates a vector from the 1950 frame to true equatorial coordinates of date, then the desired apparent source direction $\hat{S}$ is given by

$$\hat{S} = R_{pn}\hat{S}_c \tag{11}$$

The exact form of the matrix R_{pn} may be obtained from Ref. 7.

A calculation of the baseline vector $\mathbf{B}(t)$ in terms of true equatorial coordinates of date must include diurnal rotation and the motion of the Earth's instantaneous spin axis relative to the crust of the Earth (polar motion). Suppose an Earth-fixed baseline vector $\mathbf{B}_{03}$ is given in terms of an Earth-fixed coordinate system for which the z'-axis is the mean pole of 1903.0, the x'-axis is along the 1903 Greenwich meridian, and the y'-axis is 90°E. Then the baseline at time t is given by

$$\mathbf{B}(t) = R_e R_p \mathbf{B}_{03} \tag{12}$$

The matrix (Ref. 4)

$$R_p = \begin{pmatrix} 1 & 0 & -X/a \\ 0 & 1 & Y/a \\ X/a & -Y/a & 1 \end{pmatrix} \tag{13}$$

accounts for small rotations due to polar motion and rotates the Earth's crust to its proper orientation relative to the true pole of date as indicated in Fig. 2. X and Y are the coordinates of the instantaneous spin axis relative to the mean pole of 1903.0 and a is the polar radius. Positive X refers to positive displacement along the 1903.0 Greenwich meridian while positive Y refers to positive displacement toward 270°E. The matrix

$$R_e = \begin{pmatrix} \cos\alpha_G(t) & -\sin\alpha_G(t) & 0 \\ \sin\alpha_G(t) & \cos\alpha_G(t) & 0 \\ 0 & 0 & 1 \end{pmatrix} \tag{14}$$

accounts for the Earth's spin and rotates the baseline vector to its instantaneous orientation relative to true equatorial coordinates of date. The angle α_G will be called the right ascension of Greenwich and will be defined in the following manner. An Earth-fixed 1903 Greenwich meridian is defined by Greenwich and the mean pole of 1903.0. The point at which this Earth-fixed meridian crosses the true equator of date is invariant under small rotations of the Earth's crust about the x' and y' axes due to polar motion. This fact is illustrated in Fig. 2. Therefore, if the right ascension of Greenwich α_G is defined to be the right ascension of this crossing point relative to true equatorial coordinates of date, the polar motion parameters (X, Y), and α_G are uncoupled independent rotation parameters when the corresponding rotations are applied in the order indicated in Eq. (12).

Thus the time delay contains information concerning the source location, polar motion, precession and nutation,

UT1, and the baseline vector. A discussion of the sensitivity of the time delay and delay rate to all of these factors has been presented in previous work (Ref. 4).

Up to this point, the analysis has been performed in a QLG frame. In order to determine the time delay observed in antenna frames, observation times must be transformed to the rotating Earth-fixed antenna frames. Denote the time scales for antenna frames 1 and 2 by t' and t'' respectively. Since these antenna times are essentially the proper times of their respective frames, the time transformation between antenna frame and QLG frame is given by

$$t_\alpha = \gamma_1 t'_\alpha$$

where

$$\gamma_1 = (1 - v_1^2/c^2)^{-1/2} \tag{15}$$

for event α at antenna 1 and

$$t_\beta = \gamma_2 t''_\beta$$

where

$$\gamma_2 = (1 - v_2^2/c^2)^{-1/2} \tag{16}$$

for event β at antenna 2. The antenna speeds are given by $v_i = |\dot{\mathbf{x}}_i|$. We have assumed that all the clocks have been synchronized so that the time transformations are homogeneous. The effect of these transformations is to compress in time the waveform observed in the antenna frames compared to that predicted by observers in the geocentric frame.

Let t'_1 be the arrival time of a marked wave segment as seen in the frame of antenna 1 and let t''_2 be its arrival time in the frame of antenna 2. As defined previously, let t_1 and t_2 represent the corresponding arrival times at antennas 1 and 2 as observed in the QLG frame. According to the time transformations given above, these arrival times are related by the expressions $t_1 = \gamma_1 t'_1$ and $t_2 = \gamma_2 t''_2$. When the antenna teams compare arrival times, they will find the time delay is given by

$$t''_2 - t'_1 = \frac{t_2}{\gamma_2} - \frac{t_1}{\gamma_1} = \frac{\tau_g}{\gamma_2} + \frac{\gamma_1 - \gamma_2}{\gamma_2} t'_1 \tag{17}$$

where, by definition, the QLG time delay is given by $\tau_g = t_2 - t_1$. Thus, the transformation to the Earth-fixed frames introduces a time-delay contraction factor γ_2 and a linear drift

$$\frac{\gamma_1 - \gamma_2}{\gamma_2} t'_1$$

Since present VLBI time-delay measurement uncertainty is no better than one part in 10^8, a time-delay contraction of a part in 10^{12} (for $v/c \approx 10^{-6}$) is not presently observable.

With regard to the linear drift, the difference, $\gamma_1 - \gamma_2$, can be of the order of 10^{-12} if the two antennas are at considerably different latitudes. In experiments with time calibration and stability considerably better than $\Delta T/T = 10^{-12}$ (possibly an H-maser system with $\Delta T/T = 10^{-14}$), this drift would be observed as a gradual linear loss of synchronization if the time delay measurement uncertainty were sufficiently small. With a 2 MH_z recording system, the time delay could be measured with a precision of about 10 nsec (see *Section V*). With this precision, a relativistic synchronization drift of one part in 10^{-12} would be observable within several hours if the time systems possessed stability and calibration considerably better than $\Delta T/T = 10^{-12}$.

Note that the time derivative of the observed delay exhibits an additive factor, $(\gamma_1 - \gamma_2)/\gamma_2$, relative to the uncorrected delay rate, $\dot{\tau}_g$. At S-band, this additive factor can produce a constant offset of the order of 1 mHz in the observed fringe frequency (see *Section III*). This frequency offset would normally be concealed in the uncalibrated offset between the mixing frequencies at the two stations.

For simplicity, these small relativistic effects will be omitted in the analysis of the cross-correlation procedure that follows in the next section. In that analysis, no distinction will be made between antenna times and QLG time. However, the inclusion of these effects is a straightforward extension of the analysis and results in the corrected time-delay derived above.

III. Cross-Correlation for a Point Source

In the cross-correlation procedure, the radio signals recorded at the two antennas are offset by a model time delay and multiplied together. In this section, an expression for the average value of this voltage product is derived for a natural point source.

As indicated in the last section, we may assume that, for an extragalactic point source, the electric field detected at the receiver of station j is given by

$$E_j(t) = \int_0^\infty A(\omega) \exp\left(i\left[\omega t - \mathbf{k}\cdot\mathbf{x}_j(t)\right]\right) d\omega + \text{c.c.} \qquad (18)$$

where c.c. denotes complex conjugate. After being heterodyned and filtered, the recorded voltage at station j will have the form

$$V_j(t) = \int_0^\infty A(\omega)\, G_j(y_j) \exp(i\psi_j)\, d\omega + \text{c.c.} + \eta_j(t) \qquad (19)$$

where

$$y_j = \omega\left(1 - \hat{k}\cdot\dot{\mathbf{x}}_j/c\right)$$
$$\psi_j = (\omega - \omega_j)\, t - \mathbf{k}\cdot\mathbf{x}_j - \omega\tau_j + \phi_j$$

and G_j is the effective bandpass filter, ω_j is the effective mixing frequency, ϕ_j is an electronic phase shift, τ_j is the electronic time delay and $\eta_j(t)$ is instrumental noise and background radio noise.

The effective bandpass function $G_j(\Omega)$ is a complex transfer function that includes all of the phase shifts and amplitude modulation experienced by the frequency component $e^{i\Omega t}$ in its trip down the heterodyne-filter chain to baseband. With no loss in generality, the whole process may be analytically and conceptually replaced by one filter at RF followed by one effective heterodyne process (ω_j) to baseband provided that all amplitude and phase effects are included in the effective filter. The term, $\hat{k}\cdot\mathbf{v}_j$, in the argument of the filter accounts for doppler shifting. That is, the "inertial" frequency component ω will be received at frequency $\omega\left(1 - \hat{k}\cdot\mathbf{v}_j/c\right)$ and will be modulated in the heterodyne-filter chain on the basis of this initial doppler-shifted frequency.

A model time delay is given to good approximation by the expression

$$\tau_m = \hat{S}\cdot\mathbf{B}(t) + \tau_c \qquad (20)$$

where τ_c is an adjustable factor to account for clock errors and instrumental delays. The apparent source direction $\hat{S}$ and baseline $\mathbf{B}$ are calculated on the basis of the best values for UT1, station locations and source location. The apparent source position should include, at least approximately, the precession, nutation and aberration effects described in the last section. Except for τ_c, a model time delay constructed in this fashion is typically accurate to about one part in 10^5 or 10^6.

Once a model time delay has been calculated, the voltage signals may be offset and multiplied together as follows

$$V_1(t)\, V_2(t + \tau_m) =$$
$$\int_0^\infty \int_0^\infty A(\omega)\, A^*(\omega')\, G_1(y_1)\, G_2^*(y_2')\, e^{i\psi}\, d\omega\, d\omega' + \text{c.c.}$$
$$+ \int_0^\infty \int_0^\infty A(\omega)\, A(\omega')\, G_1(y_1)\, G_2(y_2')\, e^{i\psi_c}\, d\omega\, d\omega' + \text{c.c.}$$
$$+ \text{noise terms} \qquad (21)$$

where

$$y_1 = \omega\left(1 - \hat{k}\cdot\dot{\mathbf{x}}_1/c\right)$$
$$y_2' = \omega'\left(1 - \hat{k}\cdot\dot{\mathbf{x}}_2/c\right)$$
$$\psi = \mathbf{k}\cdot\mathbf{B}_r(t) + (\omega - \omega')\, t + (\omega_2 - \omega_1)\, t - \omega\tau_1 + \omega'\tau_2$$
$$- (\omega' - \omega_2)\, \tau_m + \phi \qquad (22)$$

for which

$$\mathbf{B}_r(t) \equiv \mathbf{x}_2(t + \tau_m) - \mathbf{x}_1(t) = \text{retarded baseline}$$
$$\phi \equiv \phi_1 - \phi_2$$

and ψ_c is a similar expression that, as we will see, will not be needed. By expanding about t and using Eq. (6), one can easily show that

$$\mathbf{k}\cdot\left[\mathbf{x}_2(t + \tau_m) - \mathbf{x}_1(t)\right] \approx \omega\left[\tau_g + \frac{\hat{S}\cdot\mathbf{v}_2}{c}\left(\tau_g - \tau_m\right)\right] \qquad (23)$$

Since v_2/c is of the order of 10^{-6}, and since τ_m typically differs from τ_g by only one part in 10^5, the second term may be neglected. Thus, to very good approximation,

$$\mathbf{k}\cdot\mathbf{B}_r(t) = \omega\tau_g \qquad (24)$$

and

$$\psi = \omega\tau_g + (\omega - \omega')\, t + (\omega_2 - \omega_1)\, t - \omega\tau_1 + \omega'\tau_2$$
$$- (\omega - \omega_2)\, \tau_m + \phi \qquad (25)$$

Since the exact forms of the radio signal and additive noise recorded in a particular experiment are not known, a statistical average of the voltage product is in order. An ensemble average of the voltage product will reveal long-term variations ($>>$ bandwidth^{-1}) due to factors such as the time delay, since it statistically removes short-term fluctuations ($\approx$ bandwidth^{-1}) due to both signal and noise. Furthermore, an ensemble approach provides a

formalism that sets the stage for analysis of subsequent data reduction (fringe stopping, Fourier analysis, etc.).

An average over the ensemble of all possible noise waves leads to the form

$$\langle V_1(t)\, V_2(t+\tau_m)\rangle =$$

$$\int_0^\infty \int_0^\infty \langle A(\omega)\, A^*(\omega')\rangle\, G_1(y_1)\, G_2^*(y_2')\, e^{i\psi}\, d\omega\, d\omega' + \text{c.c.}$$

$$+ \int_0^\infty \int_0^\infty \langle A(\omega)\, A(\omega')\rangle\, G_1(y_1)\, G_2(y_2')\, e^{i\psi_c}\, d\omega\, d\omega' + \text{c.c.} \tag{26}$$

where the brackets $\langle\ \rangle$ denote an ensemble average. Because the instrumental noise is uncorrelated between stations and uncorrelated with radio noise, the instrumental noise terms have zero expected value. It has been assumed that background radio noise is also uncorrelated.

In order to obtain the ensemble average of the frequency components, one must assess the statistical properties of the radio noise. The frequency spectrum of a particular member of the noise ensemble is obtained by Fourier analysis of the electric field, $E_p(t)$, measured at a fixed point in QLG coordinates.

$$A(\omega) = \frac{1}{2\pi}\int_{-\infty}^{\infty} E_p(t)\, e^{i\omega t}\, dt \tag{27}$$

For simplicity, the following derivation neglects the convergence problem associated with Fourier transforms of noise signals of "infinite" extent. Since more rigorous truncation and limit techniques (Ref. 8) do not change the essence or the result of the derivation, they have been replaced by a simpler delta function approach. An ensemble average of the frequency components is given by

$$\langle A(\omega)\, A^*(\omega')\rangle =$$

$$\frac{1}{(2\pi)^2}\int_{-\infty}^{\infty}\int_{-\infty}^{\infty} \langle E_p(t)\, E_p(t')\rangle \exp(i\omega t - i\omega' t')\, dt\, dt' \tag{28}$$

If we assume that, according to QLG observers, the radio noise is stationary (Ref. 1), we have

$$\langle E_p(t)\, E_p(t')\rangle = R(t-t') = R(\tau) \tag{29}$$

where R is the autocorrelation function for the radio noise and $\tau = t - t'$ is the standard autocorrelation delay and has no relation to the geometric time delay obtained earlier.

Hence, we obtain by change of variable

$$\langle A(\omega)\, A^*(\omega')\rangle = \frac{1}{(2\pi)^2}\int_{-\infty}^{\infty} R(\tau)\, e^{i\omega\tau}\, d\tau \times \int_{-\infty}^{\infty} e^{i(\omega-\omega')t'}\, dt'$$

$$= S_p(\omega)\, \delta(\omega - \omega') \tag{30}$$

where $S_p(\omega)$ is the power spectrum (Ref. 8) of the radio noise and $\delta(\omega - \omega')$ is the Dirac delta function. Since $A^*(\omega') = A(-\omega')$, we obtain

$$\langle A(\omega)\, A(\omega')\rangle = S_p(\omega)\, \delta(\omega + \omega') \tag{31}$$

Thus different frequency components of stationary radio noise are uncorrelated (Ref. 8).

The average voltage product, which will be called the cross-correlation function, becomes

$$r_v = \langle V_1(t)\, V_2(t+\tau_m)\rangle$$

$$= \exp[i(\omega_2 - \omega_1)t + i\omega_2\tau_m + i\phi] \times \int_0^\infty S_p(\omega)\, G_1(y_1)\, G_2^*(y_2)\, e^{i\omega\Delta\tau}\, d\omega + \text{c.c.} \tag{32}$$

where

$$\Delta\tau = \tau_g + \tau_e - \tau_m$$

$$\tau_e = \tau_2 - \tau_1$$

The $A(\omega)\, A(\omega')$ term has dropped out since $\omega = -\omega'$ is not covered in the region of integration. The derivation of this expression for the cross-correlation function requires only one assumption regarding the statistics of radio noise—the assumption of stationarity.

We may use the identity $e^{-i\omega_0\Delta\tau}\, e^{i\omega_0\Delta\tau} = 1$ to rewrite the cross-correlation function in the form

$$r_v = F(t)\, D(\Delta\tau) + \text{c.c.} \tag{33}$$

where

$$F(t) = \exp[i(\omega_2 - \omega_1)t + i\omega_2\tau_m + i\omega_0\Delta\tau + i\phi] \tag{34}$$

$$D(\Delta\tau) = \int_0^\infty S_p(\omega)\, G_1(y_1)\, G_2^*(y_2)\, e^{i(\omega-\omega_0)\Delta\tau}\, d\omega \tag{35}$$

The frequency, ω_0, is nominally the "center" of the bandpass product. We will call the function, $D(\Delta\tau)$, the time delay function and the function, $F(t)$, fast fringes.

The center frequency, ω_0, may now be selected to minimize the time dependence of the time delay function so that it makes a negligible contribution to the frequency of the cross-correlation function. That is, the fast fringe function will contain all the sinusoidal time dependence while the time delay function will be a slowly varying amplitude. Since sinusoidal dependence in the time delay function arises from the exp $[i(\omega - \omega_0)\Delta\tau]$ factor, the following analysis will be dedicated to removing the sinusoidal impact of this factor.

The transfer function product may be written in the form

$$G_1 G_2^* = |G_1|\,|G_2| \exp[i(\theta_1 - \theta_2)] = |G_1|\,|G_2|\, e^{i\Delta\theta} \tag{36}$$

where θ_1 and θ_2 represent the aggregate phase shifts of the two systems and $\Delta\theta = \theta_1 - \theta_2$. The constant part of $\Delta\theta$ can be included in ϕ. The part of $\Delta\theta$ that is linear in frequency is equivalent to an electronic delay and can be included in τ_e. The remaining nonlinear part of $\Delta\theta$ will be negligibly small if the filters are nearly ideal and/or nearly identical.

If we assume the time delay error, $\Delta\tau$, is small (as we shall see, we can do this by maximizing the time delay function), we may write

$$D \approx \int_0^\infty S_p\,|G_1|\,|G_2|\,[1 + i(\omega - \omega_0)\Delta\tau]\,d\omega \tag{37}$$

A weak time dependence is found in the amplitudes $|G_1|$ and $|G_2|$ due to doppler shifting of their arguments, which have been omitted for simplicity. Since amplitude variations in the time delay function are acceptable, we may neglect the time dependence in $|G_1|$ and $|G_2|$.

Under these conditions, we may minimize the sinusoidal content of the time delay function by requiring the second term of Eq. (37) to be zero so that

$$\omega_0 = \frac{\int S_p\,|G_1(y_1)|\,|G_2(y_2)|\,\omega\,d\omega}{\int S_p\,|G_1(y_1)|\,|G_2(y_2)|\,d\omega} \tag{38}$$

Thus, for nearly identical transfer functions and a flat power spectrum, the center frequency is the centroid of the doppler-corrected bandpass product. Under the stated conditions, this choice for ω_0 will reduce the time delay function to a slowly varying amplitude for time delay errors, $\Delta\tau$, that are small compared to the reciprocal bandwidth.

In order to illustrate the essential features of the cross-correlation function, assume both stations have the same effective square bandpass of width W. Also, suppose the systems are configured in the double sideband mode so that bandpass j is effectively centered at mixing frequency ω_j when there is no doppler shift. When there is a doppler shift D_j, bandpass j will be effectively centered at $\omega_j - D_j$. If we assume the power spectrum is flat within the bandpass, we then have for $W/\omega_0 << 1$

$$\begin{aligned} S_p(\omega)\,G_1 G_2 &= \text{constant} = K \quad \text{for } |\omega - \omega_0| < \pi W_D \\ &= 0 \quad \text{for } |\omega - \omega_0| > \pi W_D \end{aligned} \tag{39}$$

where the centroid ω_0 is given by

$$\frac{\omega_0}{2\pi} \approx \frac{f_1 + f_2}{2} - \frac{D_1 + D_2}{2} \tag{40}$$

and the effective product bandwidth W_D by

$$\begin{aligned} W_D &\approx W - |f_2 - f_1 + D_1 - D_2| \\ &\qquad \text{for } W > |f_2 - f_1 + D_1 - D_2| \\ &= 0 \text{ otherwise} \end{aligned} \tag{41}$$

where

$$f_i = \omega_i/2\pi$$

Note that the effective bandwidth W_D decreases if the mixing frequencies have not been chosen to compensate for the doppler difference. Also note that the effective receiving frequency ω_0 is a function of doppler shift.

Under these bandpass assumptions, the cross-correlation function is given by

$$\langle V_1(t)\,V_2(t + \tau_m)\rangle = 4\pi K W_D \frac{\sin[\pi W_D \Delta\tau]}{\pi W_D \Delta\tau} \cos\phi_f(t) \tag{42}$$

where

$$\phi_f(t) = (\omega_2 - \omega_1)\,t + \omega_2 \tau_m + \omega_0 \Delta\tau + \phi$$

and

$$\Delta\tau = \tau_g + \tau_e - \tau_m$$

Thus, the cross-correlation function consists of a sinusoidal factor, fast fringes, multipled by a $\sin(x)/x$ factor, the delay function. The width of the delay function is equal to the reciprocal bandwidth $1/W_D$. The frequency associated with the sinusoidal factor depends on the mixing frequency difference, $\omega_2 - \omega_1$. Generally, this difference is chosen to approximately cancel the fringe rate term $\omega_0 \dot{\tau}_g$ which is about 5000 Hz for intercontinental baselines. It is readily shown that this choice of $\omega_2 - \omega_1$ also compensates for doppler shifting and aligns the two passbands.

In general, both the fast fringes and the delay function will yield information concerning the geometric delay τ_g. The magnitude of the delay function is determined by the accuracy of the model delay τ_m and peaks for zero delay error ($\Delta\tau = 0$). Therefore, by maximizing the amplitude of the cross-correlation function, one can determine the geometric delay. Once the delay function has been optimized by selection of an accurate model delay, the fast fringes may be analyzed. Because of the $2n\pi$ ambiguity involved in the inversion of sinusoidal functions, the fringe phase ϕ_f may only be determined to within an additive constant. In effect, this means that only the time derivative of the geometric delay may be obtained from the fast fringes for one passband. Thus, the delay function can lead to a measurement of the geometric delay while the fringe phase can yield a measurement of the time derivative of the geometric delay.

IV. Cross-Correlation for an Extended Source

In this section, the cross-correlation function is derived for an extended natural source that is completely incoherent. The assumptions, definitions and derivation parallel the point-source case in *Section III*.

The radio noise generated by a very distant extended natural source may be expressed as a superposition of plane waves in the form

$$E(\mathbf{x}, t) = \int_{\hat{k}} \int_0^\infty A(\hat{k}, \omega) \exp[i\omega(t - \hat{k}\cdot\mathbf{x}/c)]\, d\omega\, d\Omega + \text{c.c.} \qquad (43)$$

where $E(\mathbf{x}, t)$ is the electric field at point x and time t. $A(\hat{k}, \omega)$ is the Fourier amplitude at frequency ω for the wave received from direction $\hat{k}$. As in *Section II*, all quantities are measured with respect to a quasi-inertial geocentric frame. The wave direction $\hat{k}$ must be expressed as a function of two parameters. If $\hat{k}$ is expressed in terms of right ascension and declination, it is given by

$$\hat{k} = -(\cos\delta\cos\alpha, \cos\delta\sin\alpha, \sin\delta) \qquad (44)$$

where α, δ are the apparent right ascension and declination relative to true equatorial coordinates of date (see *Section II*). The quantity $d\Omega$ represents a differential solid angle such as $\cos\delta\, d\alpha\, d\delta$ in the case of right ascension and declination. The term $\hat{k}$ in the argument of the Fourier amplitude stands for the two direction parameters.

The electric field detected at antenna j is given by

$$E_j(t) = E(\mathbf{x}_j(t), t) = \int_{\hat{k}} \int_0^\infty A(\hat{k}, \omega) \exp(i\omega[t - \hat{k}\cdot\mathbf{x}_j(t)/c])\, d\omega\, d\Omega + \text{c.c.} \qquad (45)$$

The voltage signal recorded at antenna j is given by the expression (see *Section III*)

$$V_j(t) = \int_{\hat{k}} \int_0^\infty A(\hat{k}, \omega)\, G_j(y_j) \exp[i(\omega t - \omega_j t - \omega\hat{k}\cdot\mathbf{x}_j(t)/c - \omega\tau_j + \phi_j)]\, d\omega\, d\Omega + \text{c.c.} + \eta_j(t) \qquad (46)$$

where

$$y_j = \omega(1 - \hat{k}\cdot\dot{\mathbf{x}}_j/c)$$

and G_j is the effective band pass filter, ω_j is the effective mixing frequency, τ_j is the electronic delay, ϕ_j is the electronic phase shift and η_j is additive noise. We have assumed that the antenna pattern is large compared to the source size and may therefore be neglected. In the cross-correlation procedure, the signals from two antennas are offset by a model time delay τ_m and multiplied together giving

$$P_V = V_1(t)\,V_2(t+\tau_m)$$

$$= \int_{\hat{k}'}\int_0^\infty \int_{\hat{k}}\int_0^\infty A(\hat{k},\omega)\,A^*(\hat{k}',\omega')\,G_1(y_1)\,G_2^*(y_2')\,e^{i\psi}\,d\omega\,d\Omega\,d\omega'\,d\Omega'$$

$$+ \int_{\hat{k}'}\int_0^\infty \int_{\hat{k}}\int_0^\infty A(\hat{k},\omega)\,A(\hat{k}',\omega')\,G_1(y_1)\,G_2(y_2')\,e^{i\psi_c}\,d\omega\,d\Omega\,d\omega'\,d\Omega'$$

$$+ \text{c.c.} + \text{noise terms} \tag{47}$$

where

$$y_1 = \omega(1 - \hat{k}\cdot\dot{\mathbf{x}}_1/c)$$

$$y_2' = \omega'(1 - \hat{k}'\cdot\dot{\mathbf{x}}_2/c)$$

$$\psi = (\omega-\omega')\,t + \omega'\,\hat{k}'\cdot\mathbf{x}_2(t+\tau_m)/c - \omega\hat{k}\cdot\mathbf{x}_1(t)/c$$
$$- \omega\tau_1 + \omega'\tau_2 + (\phi_1 - \phi_2) + (\omega_2 - \omega_1)\,t - (\omega' - \omega_2)\,\tau_m$$

and ψ_c is a similar expression that will not be needed.

An ensemble average gives

$$r_v = \langle V_1(t)\,V_2(t+\tau_m)\rangle$$

$$= \int_{\hat{k}'}\int_0^\infty \int_{\hat{k}}\int_0^\infty \langle A(\hat{k},\omega)\,A^*(\hat{k}',\omega')\rangle\,G_1 G_2^*\,e^{i\psi}\,d\omega\,d\Omega\,d\omega'\,d\Omega'$$

$$+ \int_{\hat{k}'}\int_0^\infty \int_{\hat{k}}\int_0^\infty \langle A(\hat{k},\omega)\,A(\hat{k}',\omega')\rangle\,G_1 G_2\,e^{i\psi_c}\,d\omega\,d\Omega\,d\omega'\,d\Omega' + \text{c.c.} \tag{48}$$

Since the instrumental noise is uncorrelated between stations and is uncorrelated with the radio noise, all instrumental noise terms have averaged to zero.

We will assume that the natural source is completely incoherent (Ref. 1) which means

$$\langle A(\hat{k},\omega)\,A^*(\hat{k}',\omega')\rangle = S_p(\hat{k},\omega)\,\delta(\hat{k}-\hat{k}')\,\delta(\omega-\omega') \tag{49}$$

where $S_p(\hat{k},\omega)$ is the power spectrum for direction $\hat{k}$ and $\delta(z)$ represents a Dirac delta function.[1] That is, noise waves emitted by different areas of the source are uncorrelated. Furthermore, the noise emitted by a given area of the source is stationary and therefore possesses uncorrelated frequency components (see *Section III*). Since

$$A(\hat{k},\omega) = A^*(\hat{k},-\omega)$$

the last equation implies

$$\langle A(\hat{k},\omega)\,A(\hat{k}',\omega')\rangle = S_p(\hat{k},\omega)\,\delta(\hat{k}-\hat{k}')\,\delta(\omega+\omega') \tag{50}$$

Under these assumptions, we obtain

$$\langle V_1(t)\,V_2(t+\tau_m)\rangle =$$

$$\int_{\hat{k}}\int_0^\infty S_p(\hat{k},\omega)\,G_1(y_1)\,G_2^*(y_2)\,\exp i\psi_I\,d\omega\,d\Omega + \text{c.c.} \tag{51}$$

where

$$y_1 = \omega(1 - \hat{k}\cdot\dot{\mathbf{x}}_1/c)$$

$$y_2 = \omega(1 - \hat{k}\cdot\dot{\mathbf{x}}_2/c)$$

$$\psi_I = \omega\hat{k}\cdot\mathbf{B}_r/c + \omega\tau_e + \phi + (\omega_2-\omega_1)\,t - (\omega-\omega_2)\,\tau_m$$

The retarded baseline $\mathbf{B}_r$ and the instrumental terms, ϕ and τ_e, have been defined in earlier sections. The $A(\hat{k},\omega)\,A(\hat{k}',\omega')$ term has dropped out since $\omega = -\omega'$ is not covered in the region of integration.

[1]For two particular direction parameters (β,γ) the delta function $\delta(\hat{k}-\hat{k}')$, denotes $\delta(\beta-\beta')\,\delta(\gamma-\gamma')$. Furthermore, we will require β and γ to satisfy the relation $d\beta d\gamma = d\Omega$.

Let two particular parameters β, γ define the direction vector. Suppose the brightness distribution is very narrow about some central direction $\hat{k}_a$ given by

$$\hat{k}_a = \hat{k}(\beta_a, \gamma_a) \tag{52}$$

If the brightness distribution is sufficiently narrow, we may approximate the wave direction by

$$\hat{k} = \hat{k}_a + \frac{\partial \hat{k}}{\partial \beta}\bigg|_a (\beta - \beta_a) + \frac{\partial \hat{k}}{\partial \gamma}\bigg|_a (\gamma - \gamma_a) \tag{53}$$

where the partials are evaluated at the point β_a, γ_a. We then obtain

$$r_v = \langle V_1(t)\, V_2(t + \tau_m)\rangle =$$

$$\int_0^\infty R(u, v, \omega)\, G_1(\widetilde{y_1})\, G_2^*(\widetilde{y_2}) \exp(i\psi_a)\, d\omega + \text{c.c.} \tag{54}$$

where

$$\widetilde{y_1} = \omega(1 - \hat{k}_a \cdot \dot{\mathbf{x}}_1/c)$$

$$\widetilde{y_2} = \omega(1 - \hat{k}_a \cdot \dot{\mathbf{x}}_2/c)$$

$$\psi_a = \omega \hat{k}_a \cdot \mathbf{B}_r/c + \omega\tau_e + \phi + (\omega_2 - \omega_1)\, t - (\omega - \omega_2)\, \tau_m$$

In addition,

$$R(u, v, \omega) \equiv \int_{-\infty}^{\infty}\int_{-\infty}^{\infty} S_p(\beta, \gamma, \omega) \times \exp\{2\pi i [u(\beta - \beta_a) + v(\gamma - \gamma_a)]\}\, d\beta\, d\gamma \tag{55}$$

where

$$u \equiv \frac{\partial \hat{k}}{\partial \beta}\bigg|_a \cdot \mathbf{B}_r/\lambda$$

$$v \equiv \frac{\partial \hat{k}}{\partial \gamma}\bigg|_a \cdot \mathbf{B}_r/\lambda$$

$$\lambda = 2\pi c/\omega$$

We have assumed that β and γ have been defined so that $d\beta d\gamma$ is a differential solid angle. Two approximations have been made in Eq. (54) and (55). First, the weak $\hat{k}$ dependence in the bandpass functions has been neglected so that the y_1, y_2 values have been evaluated at $\hat{k}_a$. Second, the limits of the (β, γ) integration have been extended to infinity under the assumption that the brightness distribution is very narrow and terminates the integration. We will call $R(u, v, \omega)$ the brightness transform.

If we define the geometric delay for the extended source by the expression

$$\tau_g = \frac{\hat{k}_a \cdot \mathbf{B}_r}{c} \approx \frac{\hat{k}_a \cdot \mathbf{B}(t)}{c}\left[1 - \frac{\hat{k}_a \cdot \mathbf{v}_2(t)}{c}\right]^{-1} \tag{56}$$

then the cross-correlation function for an extended source, Eq. (54), becomes

$$r_v = \exp[i(\omega_2 - \omega_1)\, t + i\omega_2 \tau_m + i\phi] \times \int_0^\infty \mathrm{RG}_1\, \mathrm{G}_2^* \exp(i\omega\Delta\tau)\, d\omega + \text{c.c.} \tag{57}$$

where

$$\Delta\tau = \tau_g + \tau_e - \tau_m$$

Note that the cross-correlation function for an extended source, Eq. (57), is identical to the point-source expression, Eq. (32), except that the power spectrum $S_p(\omega)$ is replaced by R, the Fourier transform of the brightness distribution. For this reason, remarks concerning the cross-correlation function for a point source are valid for an extended source with the understanding that the fringe amplitude includes the brightness transform. Furthermore, the time delay for an extended source, Eq. (56), is the same as the point source expression, Eq. (6), except that the source location is taken as the effective center of the brightness distribution.

The visibility function (Ref. 1) is a normalized brightness transform and is defined by

$$T(u, v, \omega) = \frac{R(u, v, \omega)}{R(0, 0, \omega)} \tag{58}$$

With this definition, the visibility function for a point source would be unity for all baselines. For a diffuse source, the visibility function would equal one for a "null" baseline and would decrease as the baseline length increased. For a symmetrical source, this decrease can be substantial for baselines satisfying

$$|\mathbf{B}_r| \gtrsim \frac{\lambda}{2\, d_s} \tag{59}$$

where d_s is the source diameter in radians and λ is the radio wavelength.

In most VLBI work, the direction parameters, β and γ, are defined in terms of right ascension α and declination δ (relative to true equatorial coordinates of date) as follows.

$$\beta = \alpha \cos \delta_a$$

$$\gamma = \delta \tag{60}$$

so that

$$d\Omega = d\beta d\gamma = \cos \delta_a \, d\alpha d\delta$$

where δ_a is the apparent declination of the center of the source relative to true equatorial coordinates of date. Note that $d\beta d\gamma$ represents a differential solid angle for this choice of β and γ provided the ranges of α and δ are very small. With these definitions and Eq. (44), we obtain

$$\left.\frac{\partial \hat{k}}{\partial \beta}\right|_a = \frac{1}{\cos \delta_a} \left.\frac{\partial \hat{k}}{\partial \alpha}\right|_a = (\sin \alpha_a, -\cos \alpha_a, 0)$$

$$\left.\frac{\partial \hat{k}}{\partial \gamma}\right|_a = \left.\frac{\partial \hat{k}}{\partial \delta}\right|_a = (\sin \delta_a \cos \alpha_a, \sin \delta_a \sin \alpha_a, -\cos \delta_a) \tag{61}$$

so that

$$u = (B_x \sin \alpha_a - B_y \cos \alpha_a)/\lambda$$

$$v = (B_x \sin \delta_a \cos \alpha_a + B_y \sin \delta_a \sin \alpha_a - B_z \cos \delta_a)/\lambda \tag{62}$$

where B_x, B_y, and B_z are the instantaneous components of the baseline vector relative to true equatorial coordinates of date. We have replaced the retarded baseline with the instantaneous baseline and will neglect the small transit-time correction. The x-y components may be expressed in the form

$$B_x = B_e \cos [\lambda_B + \alpha_G (t)]$$

$$B_y = B_e \sin [\lambda_B + \alpha_G (t)] \tag{63}$$

where B_e, λ_B are the equatorial projection and longitude of the baseline and α_G is the right ascension of Greenwich at time t. We then obtain, as in Ref. 1,

$$u = -\frac{B_e}{\lambda} \sin (\lambda_B + \alpha_G - \alpha_a)$$

$$v = \frac{B_e}{\lambda} \sin \delta_a \cos (\lambda_B + \alpha_G - \alpha_a) - \frac{B_z}{\lambda} \cos \delta_a \tag{64}$$

Note that

$$\frac{u^2}{a^2} + \frac{(v - v_0)^2}{b^2} = 1 \tag{65}$$

where

$$a = \frac{B_e}{\lambda}$$

$$b = \sin \delta_a \frac{B_e}{\lambda}$$

$$v_0 = -\cos \delta_a \frac{B_z}{\lambda}$$

The last equation indicates that the Earth's rotational motion produces an elliptical path in the u-v plane (Ref. 1). Some typical paths are illustrated in Fig. 3. Note that the sense is clockwise for negative declination and counter-clockwise for positive declination. Since right ascension is not defined for $\delta_a = \pm\pi/2$, the α, δ representation is degenerate at the poles. As illustrated in Fig. 3, the u-v path becomes a point for zero equatorial projection and a straight line parallel to the u-axis for zero declination sources. In practice, one sometimes finds that only a portion of the u-v path satisfies the condition of mutal visibility. A typical visibility region has been emphasized with cross-strokes in Fig. 3a.

The measurement of the brightness transform is assisted by the relation

$$T(-u, -v, \omega) = T^*(u, v, \omega) \tag{66}$$

That is, once the brightness transform has been determined for point (u, v), its complex conjugate will give the transform for point $(-u, -v)$.

If a sufficiently diverse set of baselines were available, the brightness transform could, in principle, be measured for enough points on the u-v plane to invert the transform and thereby obtain the brightness distribution for a given source. However, because of the limited distribution and availability of radio antennas for VLBI measurements and the substantial problems involved in the experimental determination of the phase of the brightness transform, the unique measurement of a brightness distribution is a difficult task. Therefore, distribution calculations must generally be based on incomplete data and simple models.

V. Measurement Uncertainty

This section presents a brief discussion of VLBI measurement uncertainty for delay and delay rate. The discussion, which relies on description and intuition rather than rigor, outlines the variables and limitations inherent to the VLBI cross-correlation procedure presented in *Sections II* and *III*.

The accuracy with which the delay function and the fringe phase may be exploited depends on bandwidth, integration time, antenna factors (site, efficiency, system temperature), source strength, transmission media calibration error, and time-frequency system stability. By integration time, we mean the time span over which the cross-correlation is performed in order to obtain one delay or delay rate measurement. The following discussion will specify the dependence of measurement precision on integration time T, bandwidth W, and source strength S. In addition, estimates of time-frequency errors will be given for an H-maser system. The antenna variables (size, efficiency, temperature) will implicitly refer to DSN antenna systems. Transmission media calibration errors will not be discussed, although, in practice, they are a significant source of error.

With regard to the time delay function, the precision with which the time delay may be measured is determined by the width of the time delay function and the signal-to-noise ratio. The signal-to-noise ratio increases as $S\sqrt{WT}$ while the width of the time delay curve decreases as W^{-1}. Thus the time delay precision is proportional to

$$\sigma_\tau \propto W^{-3/2}\, T^{-1/2}\, S^{-1}$$

For typical long baseline source strengths (1 f.u.)[2], the time delay can be measured with a precision of about 10 μsec with a 24 kHz bandwidth, a 700-sec integration time, and DSN antenna systems. Since this uncertainty corresponds to about a 3-km baseline change (Ref. 4), no useful geophysical information can be gained from the time delay function with this narrow-band system. Therefore, with narrow-band recording, the time delay function is regarded as an amplitude that must be maximized in order to determine the source strength and to expose the fast fringes. For a 2-MHz bandwidth with the other conditions listed above, the time delay could be measured with roughly 10 nsec (3 m) precision. These estimates of precision refer only to the uncertainty due to system noise and do not include timing system or transmission media uncertainties. With an H-maser system ($\Delta T/T \approx 10^{-14}$), the clock drift over a day would be about 1 nsec.

With regard to fast fringes, we can, in effect, only extract the time derivative of the time delay or, equivalently, the fringe frequency which is defined by

$$\nu_F = \omega_0 \frac{d\tau_g}{dt}$$

For S-band observations with a 24-kHz bandwidth, DSN antenna systems, a 700-sec integration time, and typical long baseline source strengths (1 f.u.) the fringe frequency may be measured with a precision of about 0.3 mHz. This uncertainty corresponds to about a 0.5-m baseline change (Ref. 4). Since the signal to noise ratio improves as $S\sqrt{WT}$ and the frequency uncertainty decreases as $1/T$ for Fourier transform techniques, the fringe frequency precision is proportional to

$$\sigma_\nu \propto W^{-1/2}\, T^{-3/2}\, S^{-1}$$

For a 2-MHz bandwidth with the other conditions listed above, the fringe frequency could be measured with a precision of about 25 μHz (5 cm). These fringe frequency precision estimates include only the uncertainty due to system noise and do not include transmission media uncertainty or frequency system instability. For a hydrogen maser frequency system, the frequency instability is equal to roughly 30 μHz at S-band over many hours.

VI. Summary

The VLBI cross-correlation procedure has been analyzed on the basis of plane waves generated by both a natural point source and a completely incoherent extended source. The geometric time delay for a point source has been derived on the basis of plane wave phase and expressed in terms of polar motion, aberration, precession, nutation, and diurnal rotation relative to true equatorial coordinates of date. The cross-correlation analysis includes electronic factors such as the system transfer functions and the heterodyne process. The resulting cross-correlation function is a product of an amplitude factor, the delay function, and a sinusoidal factor, the fast fringes. The cross-correlation function for a completely incoherent extended source is identical to the point source expression if the point source spectral power is replaced by the brightness transform for the extended source.

[2]One flux unit (f.u.) equals 10^{-26} W/m^2-Hz.

Acknowledgments

The author is grateful to J. L. Fanselow and J. G. Williams for many stimulating discussions concerning portions of this analysis.

References

1. Swenson, F. W., and Mathur, N. C., "The Interferometer in Radio Astronomy," *Proc. IEEE*, Vol. 56, p. 2114, 1968.

2. Bracewell, R. N., *Handbuch der Physik*, 54, Springer-Verlag, Berlin, 1962.

3. Rogers, A. E. E., "Very Long Baseline Interferometry With Large Effective Bandwidth for Phase-Delay Measurements," *Radio Sci.*, Vol. 5, No. 10, pp. 1239–1248, October 1970.

4. Williams, J. G., "Very Long Baseline Interferometry and Its Sensitivity to Geophysical and Astronomical Effects," in *The Deep Space Network*, Space Programs Summary 37-62, Vol. II, pp. 49–55. Jet Propulsion Laboratory, Pasadena, Calif., March 31, 1970.

5. Fanselow, J. L., et al., "The Goldstone Interferometer for Earth Physics," in *The Deep Space Network*, Technical Report 32-1526, Vol. V, pp. 45–57. Jet Propulsion Laboratory, Pasadena, Calif., Oct. 15, 1971.

6. Jackson, J. D., "Classical Electrodynamics," p. 357, John Wiley & Sons, New York, 1962.

7. Melbourne, W. G., et al., "Constants and Related Information for Astrodynamic Calculations, 1968," Technical Report 32-1306. Jet Propulsion Laboratory, Pasadena, Calif., July 15, 1968.

8. Davenport, W. B., and Root, W. L., "Random Signals and Noise," p. 94, McGraw-Hill Book Co., New York, 1950.

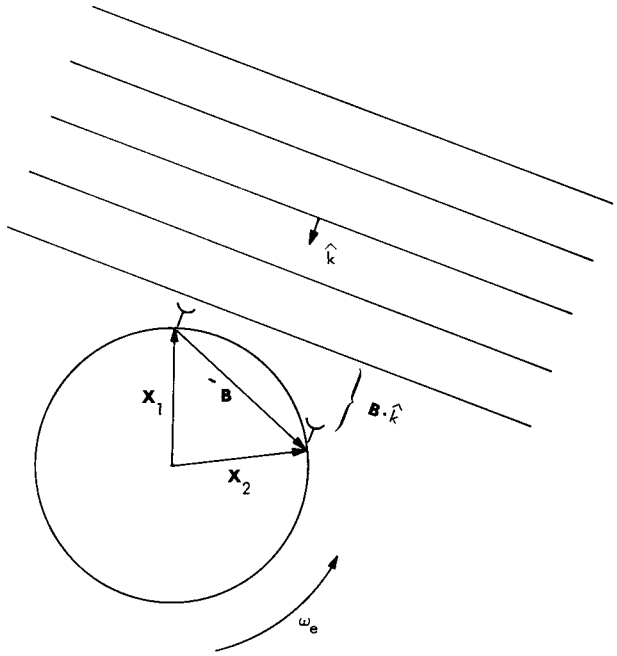

Fig. 1. VLBI geometry

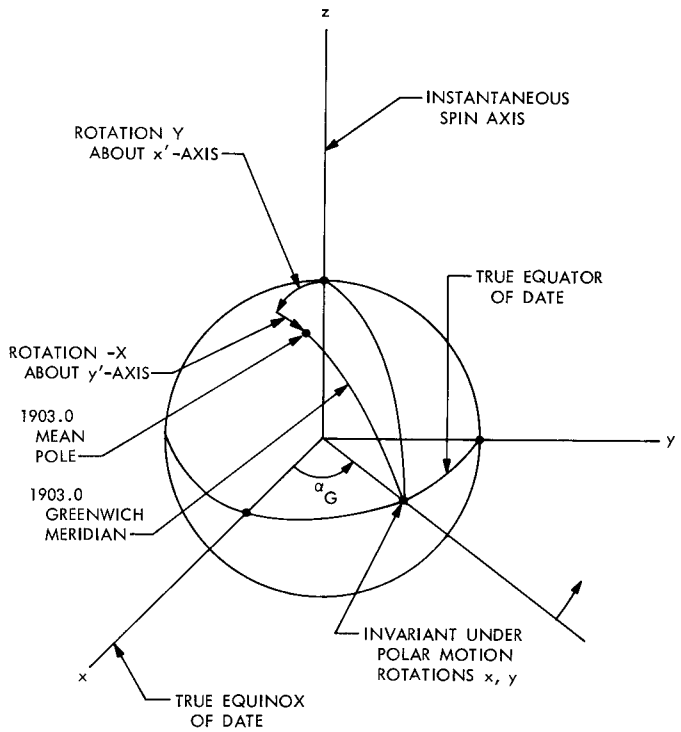

Fig. 2. Schematic of Earth crust orientation parameters X, Y, and α_G

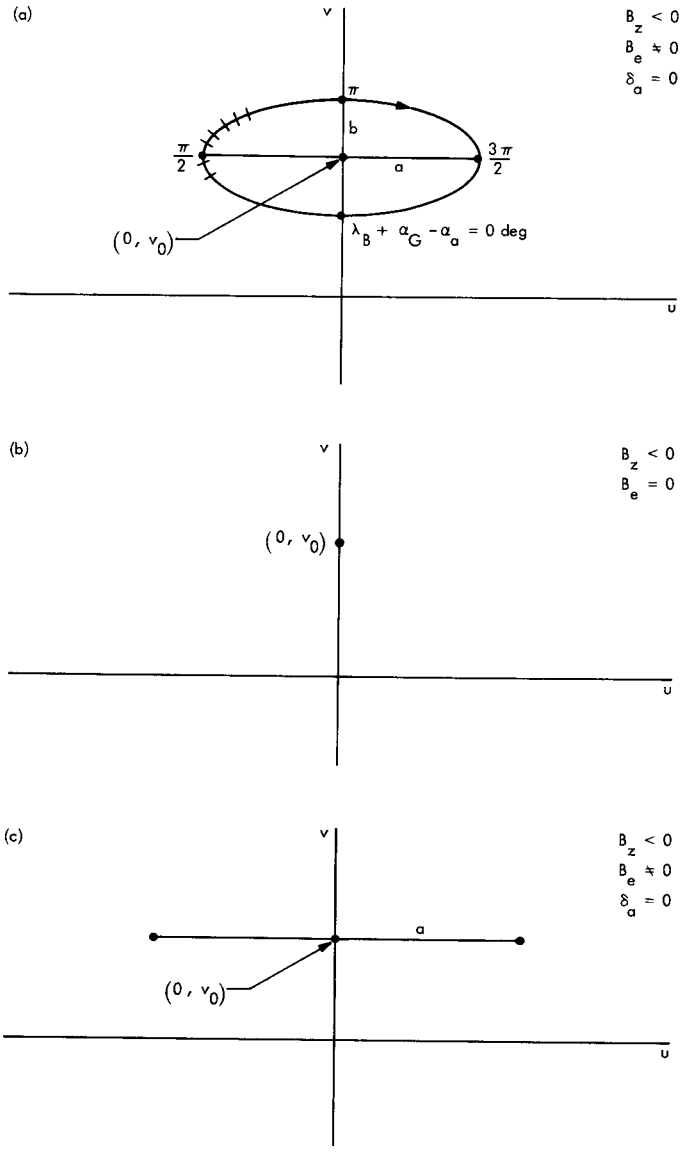

Fig. 3. Examples of diurnal paths in the *u-v* plane